

Furancarboxylate Coordination Polymers of Gd^{3+} and Eu^{3+} : Synthesis, Structural Variations, and Biological Properties

M. A. Uvarova^a, *, I. A. Lutsenko^a, M. A. Shmelev^a, O. B. Bekker^b, M. A. Kiskin^a, and I. L. Eremenko^a

^a Kurnakov Institute of General and Inorganic Chemistry, Russian Academy of Sciences, Moscow, Russia

^b Vavilov Institute of General Genetics, Russian Academy of Sciences, Moscow, Russia

*e-mail: yak_marin@mail.ru

Received January 9, 2023; revised January 17, 2023; accepted January 17, 2023

Abstract—A series of polymer complexes of $\text{Gd}^{(III)}$ and $\text{Eu}^{(III)}$ with 3-furancarboxylic (HFur) and 5-nitro-2-furancarboxylic (HNfur) acids differed in the composition and coligands presented by solvent molecules ($\text{CH}_3\text{OH}/\text{C}_2\text{H}_5\text{OH}/\text{H}_2\text{O}$) is synthesized: $[\text{Gd}(\text{Fur})_3(\text{CH}_3\text{OH})(\text{C}_2\text{H}_5\text{OH})]_n$ (**I**), $[\text{Gd}(\text{Nfur})_3(\text{CH}_3\text{OH})_2]_n$ – CH_3CN (**II**), $[\text{Eu}(\text{Fur})_3(\text{C}_2\text{H}_5\text{OH})]_n$ (**III**), and $[\text{Eu}(\text{Nfur})_3(\text{H}_2\text{O})_2]_n$ – $3\text{CH}_3\text{CN}$ (**IV**). According to the X-ray diffraction (XRD) data, all complexes are 1D coordination polymers in which the lanthanide cation has the coordination number 8 (LnO_8) to form the environment as a doubly augmented triangular prism (**I**, **II**) or a square antiprism (**III**, **IV**). The supramolecular levels of the polymers are stabilized due to intra- and intermolecular hydrogen bonds between the coordinated solvent molecules and O atoms of the chelate-bound anions of the acid and via two types of noncovalent C–H...O and N–O... π interactions that significantly contribute to an additional stabilization of the crystal packings. The biological properties of complexes **I**, **II**, and **IV** are studied with respect to the model nonpathogenic strain *Mycobacterium smegmatis*.

Keywords: rare-earth element complexes, gadolinium(III), europium(III), 3-furancarboxylic acid, 5-nitro-2-furancarboxylic acid, crystal structure, coordination polymers

DOI: 10.1134/S1070328423600122

INTRODUCTION

Investigation of routes for the formation and isolation of rare-earth element (REE) coordination compounds is an actively developed area caused by attractive physicochemical properties of coordination derivatives of lanthanides, in particular, luminescence, unusual magnetic characteristics, for instance, the manifestation of properties of single-molecule magnets [1–5] or a possibility of using these molecular architectures as precursors for the formation of films and coatings on various supports [6]. Some REE chelates find use in medicine as contrast agents in magnetic resonance tomography (e.g., gadolinium and samarium drugs) and can be applied as substances with antibacterial properties [7–13]. In addition, REE ions, for example, Nd^{3+} , Sm^{3+} , or Yb^{3+} , are used for luminescence *in vivo* visualization due to their ability to emit in the near-IR range. This property makes it possible to detect such molecules via the animal tissue of a significant thickness [14]. In fact, similar substances simultaneously combining pronounced luminescence (phosphorescence) properties and biological activity are promising for the use as bioactive lumophores for both visualization and treatment, which is presently very topical trend of chemical biomedical studies.

The *d*-metal complexes with different furancarboxylic acids and N-donor ligands were studied and their biological activity was established *in vitro* against the model nonpathogenic strain *M. smegmatis* [15–20] and test SKOV3 cancer line (ovary adenocarcinoma) [21]. In this case, the $\text{Tb}^{(III)}$, $\text{Ho}^{(III)}$, $\text{La}^{(III)}$, and $\text{Eu}^{(III)}$ complexes with 2-furancarboxylic acid demonstrated perspective luminescence properties [22–28]. However, this series contains no REE compounds with other furancarboxylic acids (HFur, HNfur), which substantially impedes the selection of bioactive REE-bearing compounds for further biomedical studies and, possibly, for their applications in practice.

The purpose of this work is to develop procedures for the synthesis of gadolinium(III) and europium(III) complexes with Fur[–] and Nfur[–] anions, to determine their structures, and to study the biological properties *in vitro* against the model nonpathogenic strain *M. smegmatis*.

EXPERIMENTAL

The complexes were synthesized in air using the following solvents (without additional purification): acetonitrile (special purity grade, Khimmed), ethanol, and methanol. The following commercially available

reagents were used for the synthesis: HFur (98%, Acros), HNfur (98%, Acros), gadolinium acetate hydrate (Acros), and europium acetate hydrate (Acros). Elemental analysis was conducted on an automated Carlo Erba EA 1108 C,H,N analyzer. IR spectra were recorded on a Perkin-Elmer Spectrum 65 FT-IR spectrophotometer by the attenuated total internal reflectance (ATR) method in a frequency range of 400–4000 cm^{−1}.

The biological activity was determined in the *M. smegmatis mc² 155* test system by the paper disk method. The inhibition zone of growth of the strain, which was seeded with a lawn on an agar medium, around the paper disks containing the substance in different concentrations was detected. The bacteria washed from Petri dishes with the M-290 Tryptone soya agar medium (Himedia) were grown overnight in the Lemco-TW liquid medium (Lab Lemco' Powder 5 g L^{−1} (Oxoid), Peptone special 5 g L^{−1} (Oxoid), NaCl 5 g L^{−1}, Tween-80) at 37°C to the logarithmic mean growth phase at the absorbance OD600 = 1.5 and mixed with the molten M-290 agar medium in a ratio 1 : 9 : 10 (culture: Lemco-TW: M-290). The culture was incubated at 37°C for 24 h. The MIC (minimum inhibitory concentration) was considered to be the concentration of the substance at which the growth inhibition zone is minimum.

Synthesis of [Gd(Fur)₃(CH₃OH)(C₂H₅OH)]_n (I). A weighed sample of HFur (0.22 g, 2 mmol) was added to a solution of Gd(OAc)₃·3H₂O (0.1 g, 0.4 mmol) in methanol (10 mL), and the mixture was stirred at 60°C for 1 h. Ethanol (5 mL) was added to the resulting solution, and the reaction mixture was stored at room temperature for 2 days. Formed colorless crystals were separated from the mother liquor. The yield of compound I was 0.17 g (78%).

For C₁₈H₁₉O₁₁Gd
Anal. calcd., % C, 38.02 H, 3.36
Found, % C, 38.19 H, 3.41

IR (ATR; v, cm^{−1}): 3147 w, 2970 w, 1667 m, 1557 s, 1508 s, 1424 s, 1368 s, 1306 m, 1181 m, 1073 w, 920 w, 890 m, 778 s, 676 w, 614 m, 549 m, 463 s.

Synthesis of [Gd(Nfur)₃(CH₃OH)₂]_n·CH₃CN (II). A weighed sample of HNfur (0.3 g, 2 mmol) was added to a solution of Eu(OAc)₃·3H₂O (0.1 g, 0.4 mmol) in methanol (10 mL), and the mixture was stirred at 60°C for 1 h. Acetonitrile (5 mL) was added to the resulting solution, and the reaction mixture was stored at room temperature for 2 days. Formed colorless crystals were

decanted from the mother liquor. The yield of compound II was 0.18 g (80%).

For C₁₉H₁₆N₄O₁₇Gd

Anal. calcd., %	C, 31.27	H, 2.21	N, 7.68
Found, %	C, 31.43	H, 2.44	N, 7.58

IR (ATR; v, cm^{−1}): 3129 w, 2971 m, 1677 m, 1595 s, 1569 s, 1530 s, 1486 m, 1409 s, 1335 s, 1212 m, 1085 w, 1041 m, 1022 m, 960 w, 879 w, 836 w, 779 s, 737 m, 593 w, 516 w, 485 s, 421 m.

Synthesis of [Eu(Fur)₃(C₂H₅OH)₂]_n (III). A weighed sample of HFur (0.22 g, 2 mmol) was added to a solution of Eu(OAc)₃·3H₂O (0.1 g, 0.4 mmol) in methanol (10 mL), and the mixture was stirred at 60°C for 1 h. Ethanol (5 mL) was added to the resulting solution, and the reaction mixture was stored at room temperature for 2 days. Formed colorless crystals were decanted from the mother liquor. The yield of compound III was 0.2 g (87%).

For C₁₉H₂₁O₁₁Eu

Anal. calcd., %	C, 39.53	H, 3.67
Found, %	C, 39.34	H, 3.44

IR (ATR, v, cm^{−1}): 3370 w, 3058 w, 1605 s, 1558 s, 1543 s, 1477 s, 1415 s, 1400 s, 1367 s, 1220 m, 1192 m, 1140 w, 1078 w, 1043 w, 1009 m, 883 w, 848 m, 814 m, 781 s, 754 s, 725 s, 668 w, 616 m, 596 m, 546 w, 459 s.

Synthesis of [Eu(Nfur)₃(H₂O)₂]_n·3CH₃CN (IV). A weighed sample of HNfur (0.3 g, 2 mmol) was added to a solution of Eu(OAc)₃·3H₂O (0.1 g, 0.4 mmol) in methanol (10 mL), and the mixture was stirred at 60°C for 1 h. Acetonitrile (5 mL) was added to the resulting solution, and the reaction mixture was stored at room temperature for 7 days. Formed colorless crystals were decanted from the mother liquor. The yield of compound IV was 0.2 g (84%).

For C₂₁H₁₉N₆O₁₇Eu

Anal. calcd., %	C, 32.36	H, 2.46	N, 10.78
Found, %	C, 32.26	H, 2.14	N, 10.98

IR (ATR, v, cm^{−1}): 3404 m, 3032 m, 2969 m, 1671 m, 1597 s, 1561 s, 1566 s, 1535 s, 1488 m, 1465 w, 1410 s, 1331 s, 1210 m, 1085 m, 1061 m, 1041 m, 1022 m, 991 w, 877 w, 860 w, 836 w, 778 s, 731 m, 590 w, 485 s, 418 m.

XRD of compounds I–IV was carried out on a Bruker ApexII diffractometer (MoK_α, $\lambda = 0.71073$ Å, graphite monochromator, CCD detector). A semiempirical absorption correction was applied using the SADABS program [29]. The structures were solved using the ShelXT program [30] and refined by full-matrix least squares using the Olex2 program [31] in

Table 1. Selected crystallographic data and experimental and structure refinement parameters for compounds **I–IV**

Parameters	Value			
	I	II	III	IV
Empirical formula	$\text{C}_{18}\text{H}_{19}\text{O}_{11}\text{Gd}$	$\text{C}_{19}\text{H}_{17}\text{N}_4\text{O}_{17}\text{Gd}$	$\text{C}_{19}\text{H}_{21}\text{O}_{11}\text{Eu}$	$\text{C}_{21}\text{H}_{19}\text{N}_6\text{O}_{17}\text{Eu}$
FW	568.58	730.61	577.32	779.38
Crystal system	Triclinic	Monoclinic	Triclinic	Triclinic
Space group	$P\bar{1}$	$P2_1/c$	$P\bar{1}$	$P\bar{1}$
$a, \text{\AA}$	9.6981(11)	12.941(2)	9.568(7)	9.7002(3)
$b, \text{\AA}$	9.7221(11)	9.5419(14)	9.613(6)	10.7733(3)
$c, \text{\AA}$	11.1393(13)	22.345(3)	11.356(9)	14.4037(4)
α, deg	87.654(4)	90	83.49(3)	98.574(2)
β, deg	83.242(4)	104.179(5)	89.58(3)	93.192(2)
γ, deg	76.332(4)	90	76.56(2)	93.622(2)
$V, \text{\AA}^3$	1013.4(2)	2675.2(7)	1009.1(13)	1482.20(7)
Z	2	4	2	2
$\rho_{\text{calc}}, \text{g/cm}^3$	1.863	1.814	1.900	1.746
$\mu(\text{Mo}K_{\alpha}), \text{cm}^{-1}$	3.331	2.566	3.169	2.203
$2\theta_{\text{max}}, \text{deg}$	24.712	24.406	24.711	25.998
$F(000)$	558	1436	572	772
Number of reflections	6919	11920	5401	27086
Independent reflections	3425	4373	3346	5806
R_{int}	0.0467	0.0866	0.0550	0.0501
Observed reflections with $I > 2\sigma(I)$	3068	2940	3123	5361
GOOF	1.090	1.031	1.078	1.058
$R_1, wR_2 (I > 2\sigma(I))$	0.0544, 0.1430	0.0587, 0.1410	0.0618, 0.1571	0.0278, 0.0633
$\Delta\rho_{\text{max}}, \rho_{\text{min}}, \text{e}/\text{\AA}^3$	3.444/−2.172	1.172/−1.910	4.372/−3.577	1.268/−0.850

the anisotropic approximation for non-hydrogen atoms. The hydrogen atoms of the water molecules were localized from the difference Fourier syntheses, positions of other hydrogen atoms were calculated geometrically, and all of them were refined in the isotropic approximation by the riding model. The geometries of polyhedra of the metal atoms were deter-

mined using the SHAPE 2.1 program [32]. Selected crystallographic data and refinement parameters for compounds **I–IV** are given in Table 1.

The full set of XRD parameters was deposited at the Cambridge Crystallographic Data Centre (CIF files CCDC nos. 2232748 (**I**), 2232749 (**II**), 2232751 (**III**), and 2232750 (**IV**); deposit@ccdc.cam.ac.uk).

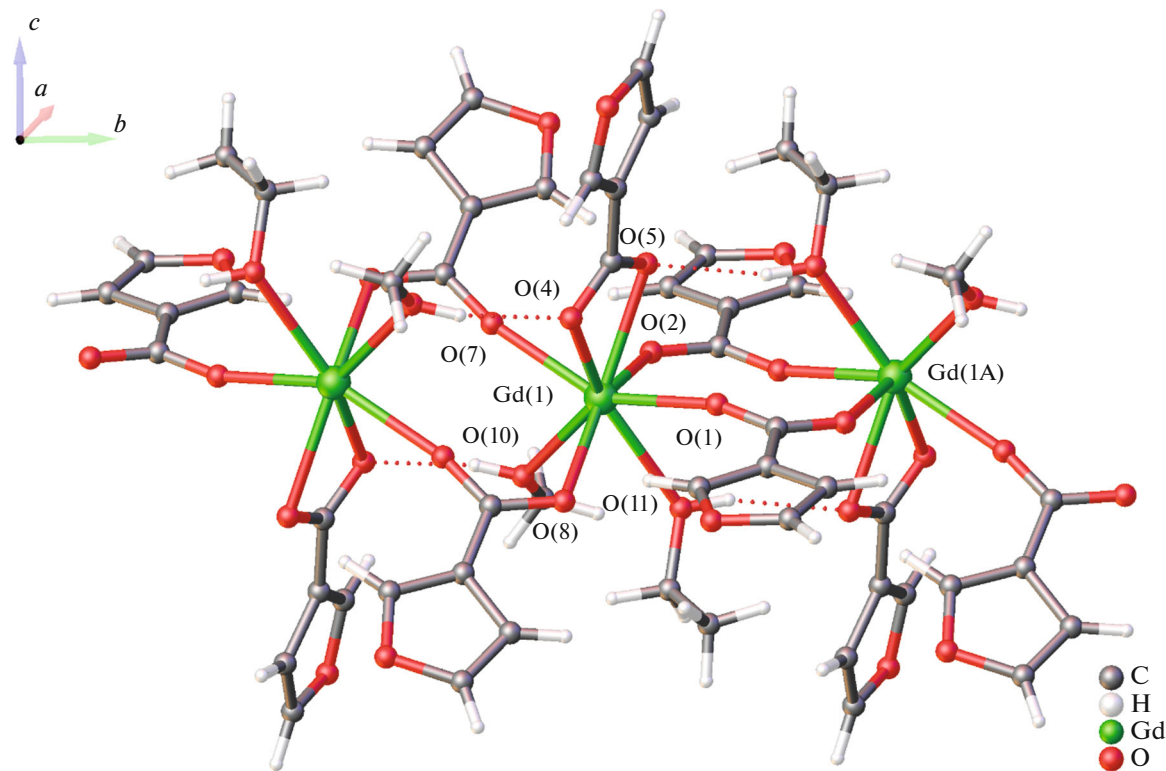


Fig. 1. Fragment of the polymer chain in compound **I**. Dashed lines show the system of hydrogen bonds.

RESULTS AND DISCUSSION

The exchange reaction of gadolinium acetate hydrate with HFur (3 mol) in methanol at 60°C for 30 min results in the full exchange the anions and formation of a finely crystalline phase, the recrystallization of which from an ethanol–methanol (1 : 1) mixture affords single crystals of $[\text{Gd}(\text{Fur})_3 \cdot (\text{CH}_3\text{OH})(\text{C}_2\text{H}_5\text{OH})]_n$ (**I**) suitable for XRD. The reaction of HNfur with gadolinium acetate hydrate in methanol, under similar conditions with the addition of acetonitrile, leads to the formation of $[\text{Gd}(\text{Nfur})_3(\text{CH}_3\text{OH})_2]_n \cdot \text{CH}_3\text{CN}$ (**II**) being, as com-

ound **I**, a 1D coordination polymer. Similar reactions for europium acetate hydrate under the same conditions lead to polymer complexes $[\text{Eu}(\text{Fur})_3 \cdot (\text{C}_2\text{H}_5\text{OH})]_n$ (**III**) and $[\text{Eu}(\text{Nfur})_3(\text{H}_2\text{O})_2]_n \cdot 3\text{CH}_3\text{CN}$ (**IV**). Thus, the variations with the solvents showed that the Gd^{3+} cations can coordinate simultaneously molecules of alcohols: methanol and ethanol (**I**)/methanol (**II**), whereas the Eu^{3+} cations tend to form bonds with molecules of ethanol (**III**) or water (**IV**) under equivalent synthetic conditions.

Complexes **I** and **III** crystallize in the triclinic space group $P\bar{1}$ with the inversion center between the

Table 2. Selected bond lengths (Å) for compounds **I**–**IV**

Bond length, Å	I	II	III	IV
	Gd		Eu	
Ln–O (Fur)	2.321(6)–2.497(6)	2.299(7)–2.394(6)	2.265(5)–2.526(6)	2.311(2)–2.527(2)
Ln–O (solv)	2.465(6), 2.494(6)	2.467(7), 2.524(7)	2.282(6), 2.368(6)	2.423(2), 2.437(2)
Ln...Ln	4.642(1), 5.114(1)	4.457(1), 5.099(1)	4.560(3), 5.070(3)	4.903(1), 4.913(1)

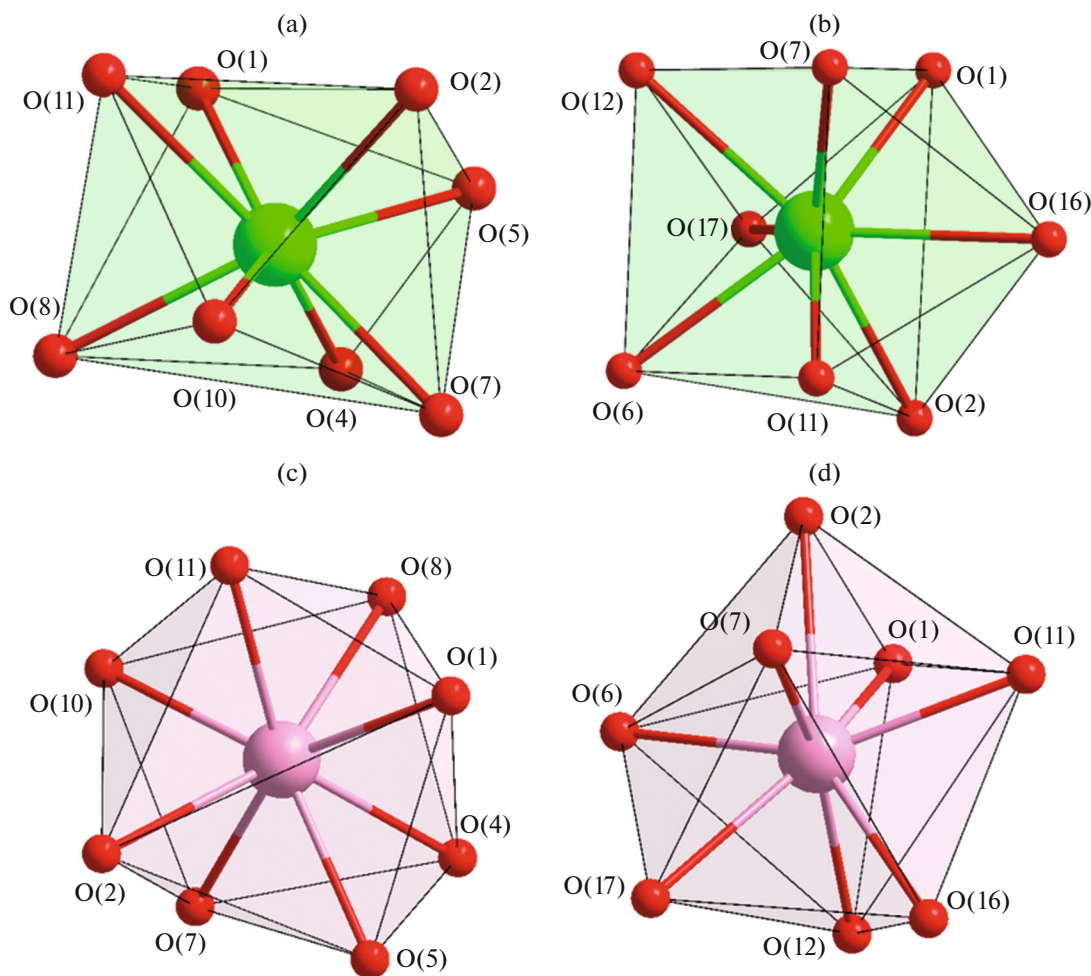


Fig. 2. Polyhedra of the REE ions (Gd is green, Eu is pink) in the structures of complexes (a) **I**, (b) **II**, (c) **III**, and (d) **IV**.

$\text{Ln}(1)$ and $\text{Ln}(1\text{A})$ ions. The REE ions in the structures of compounds **I** (Fig. 1) and **III** coordinate four bridging Fur^- anions resulting in the formation of linear polymer chains of similar structure directed along the b axis. Each lanthanide ion additionally coordinates one chelate-bound Fur^- anion and two solvent molecules thus building up its environment to a doubly augmented triangular prism in the case of the Gd^{3+} ion (Fig. 2a, GdO_8 , $\text{CShM} = 1.700$ [32]) or to a square antiprism in the case of the Eu^{3+} ion (Fig. 2c, EuO_8 , $\text{CShM} = 1.682$). On going from Gd^{3+} to Eu^{3+} , an insignificant elongation of the $\text{Ln}-\text{O}$ bonds in complexes **I** and **III** and shortening of the $\text{Ln}...\text{Ln}$ distances in the polymer chain are observed (Table 2). Interestingly, among the presented complexes, complex **III** exhibits the shortest bonds between Eu^{3+} and solvent (ethanol) molecules (2.282(6), 2.368(6) Å; Table 2). According to the Cambridge Structural Database (CSD), the lanthanide compounds similar

to complexes **I** and **III** were synthesized for benzoic [33, 34] and 3-nitrobenzoic [35] acid anions.

Compounds **II** and **IV** of different structures were synthesized for $\text{Eu}(\text{III})$ and $\text{Gd}(\text{III})$ with Nfur^- anions under similar conditions. For instance, complex **II** (Fig. 3) crystallizes in the monoclinic space group $P2_1/c$ with the inversion center between the $\text{Gd}(1)$ and $\text{Gd}(1\text{A})$ ions. Each Gd^{3+} ion coordinates six Nfur^- anions to form a polymer chain directed along the b axis. The Gd^{3+} ions in the polymer chain structure build up their environments to a doubly augmented triangular prism (Fig. 2b, GdO_8 , $\text{CShM} = 0.749$) due to the coordination of the O atoms of two MeOH molecules. According to the CSD data, several complexes with the structures similar to that of complex **II** with anions of 4-pyridine-carboxylic [36], 3,5-dinitrobenzoic [37], and trichloroacetic [38] acids were described.

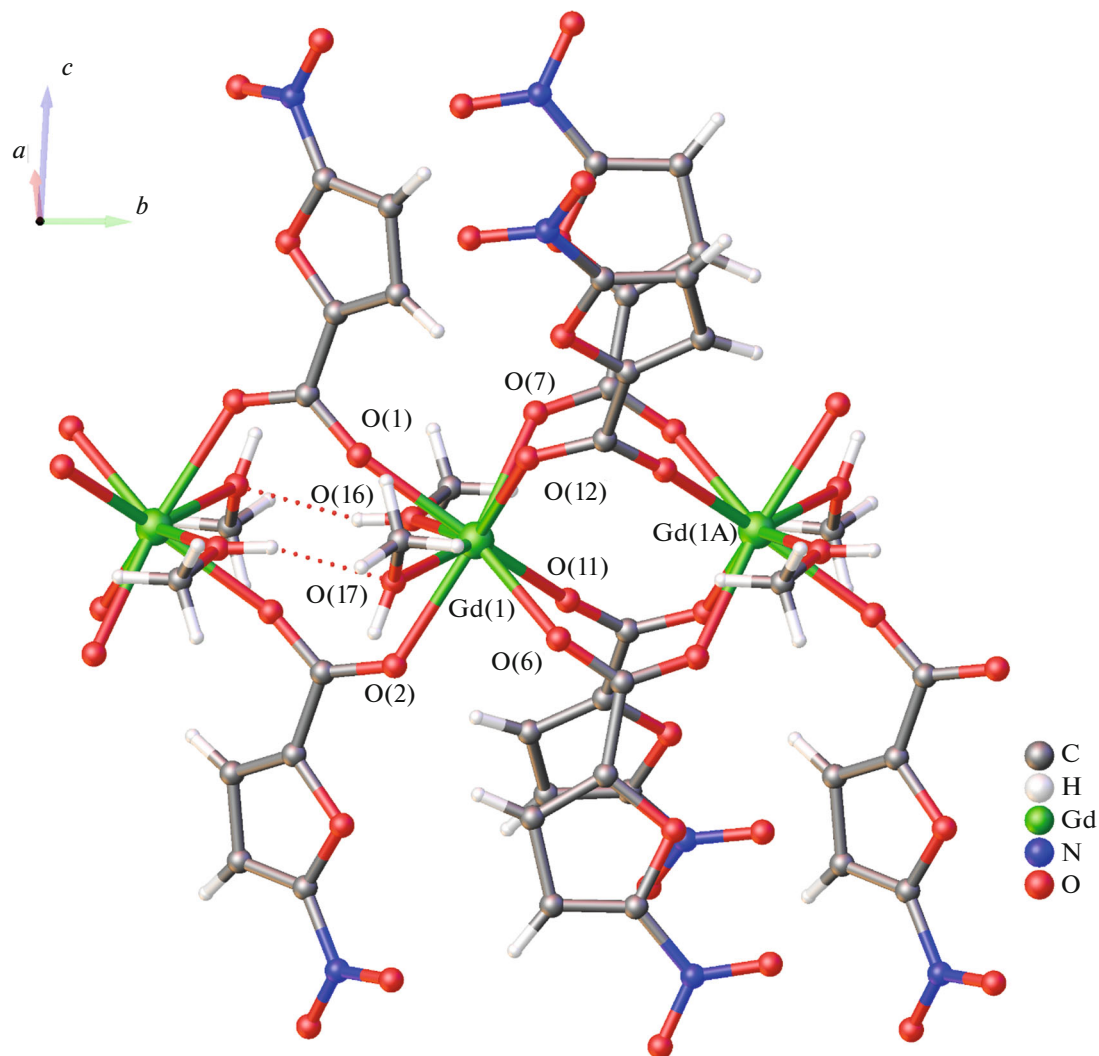


Fig. 3. Fragment of the polymer chain in compound **II**. Dashed lines show the system of hydrogen bonds. Solvate molecules are omitted.

Complex **IV** crystallizes in the triclinic space group $P\bar{1}$ with the inversion center between the Eu(1) and Eu(1A) ions. Unlike compound **II**, where each Nfur⁻ anion performs the bridging function, the polymer chain of compound **IV** is formed of two bridging Nfur⁻ anions, and the third anion is coordinated to the metal ion via the chelate mode (Fig. 4). The Eu³⁺ cation builds up its environment to a square antiprism due to the coordination of two water molecules (Fig. 2d, EuO₈, CShM = 2.066). Selected bond lengths for complexes **II** and **IV** are given in Table 2. Distinctive features of aqua complex **IV** are the increased Eu...Eu distances (4.903(1), 4.913(1) Å; Table 2) among the compounds discussed.

The packings of complexes **I**–**IV** exhibit an additional stabilization of the polymer chain due to the formation of hydrogen bonds between the coordinated

solvent molecules and O atoms of the chelate-bound acid anion (Table 3). Noncovalent interactions C–H...O are also formed to stabilize the supramolecular polymer layer (Table 3). The use of anions of 5-nitro-2-furancarboxylic acid in the case of complexes **II** and **IV** leads to the formation of additional noncovalent interactions N–O...π (Table 4), which considerably contribute to the stabilization of the crystal packings of the synthesized complexes. Solvate acetonitrile molecules incorporate into the crystal lattices of complexes **II** and **IV** due to the C–H...N and C–H...O interactions (Table 3).

The antibacterial activity of compounds **I**, **II**, and **IV** was determined toward the nonpathogenic strain *M. smegmatis*. (Compound **III** is an isostructural analog of compound **I** and, hence, its biological activity was not studied.) It is known that the resistance of

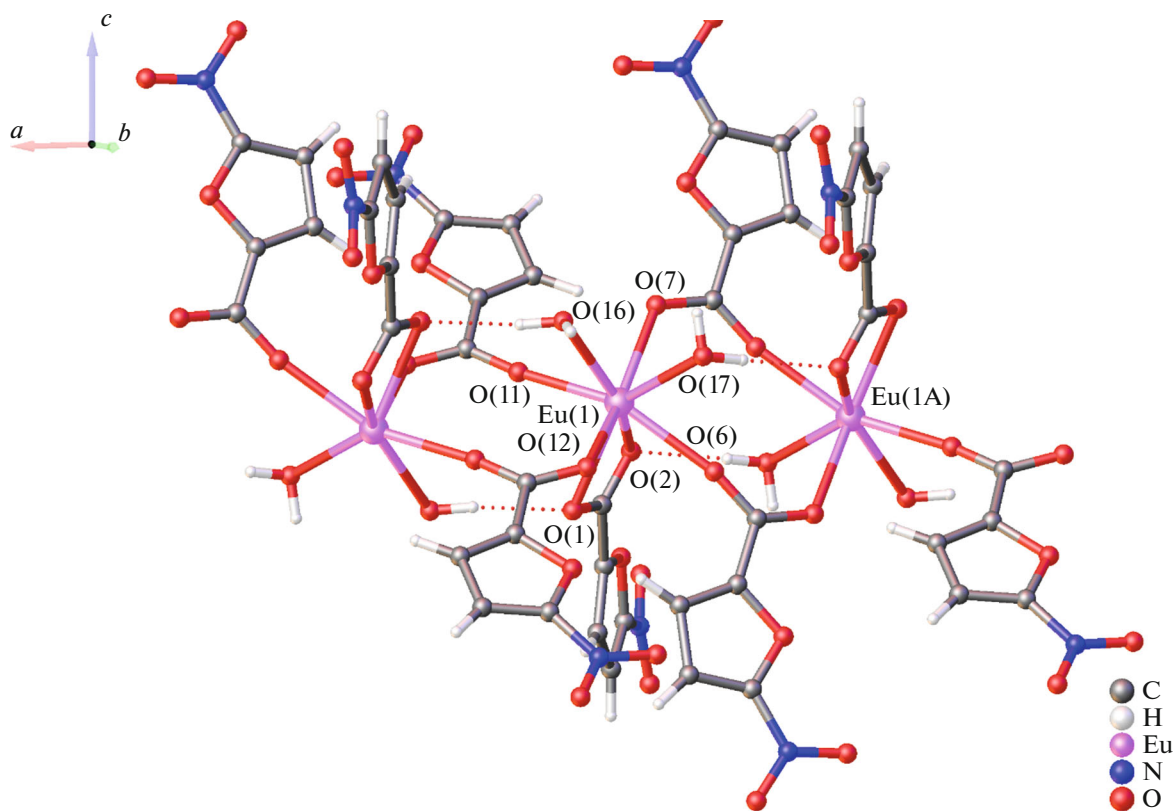


Fig. 4. Fragment of the polymer chain in compound **IV**. Dashed lines show the system of hydrogen bonds. Solvate molecules are omitted.

mycobacteria to chemotherapeutic agents is related to a low permeability of the mycobacterial cell wall and its unusual structure. *M. smegmatis* are rapidly growing nonpathogenic bacteria and, therefore, are used as the model organism for slowly growing bacteria *M. tuberculosis* and for the primary screening of antiphthisic drugs. As follows from the data in Table 5, complexes **I**, **II**, and **IV** ($\text{MIC} > 1000 \text{ nmol/disk}$) are poorly active compared to reference substances Isoniazid (INH) and Rifampicin (Rif), unlike individual furancarboxylic acids, whose values of MIC are reliably higher than those of the complexes, which indicates a decrease in the bioefficiency of the substances against the mycobacterial strain during complex formation. At the same time, we have found [14–20] that the transition metal (copper(II), zinc(II), cobalt(II, III), nickel(II), and iron(II)) complexes with furoate anions exhibit biological activity against *M. smegmatis*, which significantly increases upon the introduction into the complex of N-donor ligands, in particular, 1,10-phenanthroline or 2,2'-bipyridine. Possibly, the synthesis of adducts of the discussed complexes and, as a consequence, the transformation of polymers into molecular compounds would enhance the biological accessibility of substances for mycobacterial cells.

Thus, four 1D coordination polymers of gadolinium(III) and europium(III) in which the lanthanide

cations are bound by the bridging furoate anions were synthesized. The supramolecular level is stabilized due to numerous hydrogen bonds and noncovalent interactions joining the coordinately bound chains into the single polymer motif. The study of the biological properties of the complexes showed a low bioactivity against the nonpathogenic strain *M. smegmatis*.

ACKNOWLEDGMENTS

XRD, IR spectroscopy, and C, H, N, S analyses were carried out using the equipment of the Center for Collective Use of Physical Methods of Investigation at the Kurnakov Institute of General and Inorganic Chemistry (Russian Academy of Sciences) supported by the state assignment of the Kurnakov Institute of General and Inorganic Chemistry (Russian Academy of Sciences) in the area of basic research.

FUNDING

This work was supported by the Ministry of Science and Higher Education of the Russian Federation in terms of the state assignment of the Kurnakov Institute of General and Inorganic Chemistry (Russian Academy of Sciences).

Table 3. Geometric parameters of hydrogen bonds in the crystal packings of compounds I–IV

D–H...A	Distance, Å				Angle D–H...A, deg
	D–H	symmetry code	H...A	D...A	
I					
O(10)–H(10)...O(4)	0.84	$1-x, 1-y, 1-z$	1.92	2.751(8)	169
O(11)–H(11)...O(1)	0.84	$1-x, 2-y, 1-z$	2.55	3.085(9)	123
C(3)–H(3)...O(8)	0.95	$1-x, 1-y, 1-z$	2.39	3.241(12)	149
C(9)–H(9)...O(3)	0.95	$x, y, 1+z$	2.55	3.407(13)	150
C(13)–H(13)...O(2)	0.95	$1-x, 2-y, 1-z$	2.54	3.350(11)	144
C(16)–H(16B)...O(11)	0.98		2.57	3.169(14)	119
II					
O(16)–H(16)...O(1)	0.853(16)	$1-x, -y, 1-z$	2.36(7)	2.911(10)	123(7)
O(17)–H(17)...N(4)	0.87(4)		1.98(4)	2.813(13)	161(5)
C(3)–H(3)...O(12)	0.93	$1-x, 1-y, 1-z$	2.47	3.323(12)	153
C(4)–H(4)...O(4)	0.93	$2-x, 1/2+y, 3/2-z$	2.50	3.423(14)	169
C(9)–H(9)...O(4)	0.93	$1-x, -y, 1-z$	2.47	3.176(14)	133
C(14)–H(14)...O(10)	0.93	$-x, -1/2+y, 1/2-z$	2.56	3.400(14)	151
C(19)–H(19B)...O(14)	0.96	$-x, -1/2+y, 1/2-z$	2.56	3.345(17)	144
C(19)–H(19C)...O(9)	0.96	$x, -1+y, z$	2.44	3.135(17)	129
III					
O(10)–H(10)...O(4)	0.84	$1-x, 2-y, 1-z$	2.07	2.822(8)	148
O(11)–H(11)...O(5)	0.84	$1-x, 1-y, 1-z$	1.90	2.689(8)	156
C(3)–H(3)...O(8)	0.95	$1-x, 2-y, 1-z$	2.38	3.171(11)	141
C(9)–H(9)...O(9)	0.95	$x, y, 1+z$	2.46	3.346(14)	155
C(15)–H(15)...O(2)	0.95	$1-x, 1-y, 1-z$	2.40	3.251(11)	149
C(16)–H(16B)...O(11)	0.99		2.55	3.094(11)	114
C(17)–H(17B)...O(2)	0.98	$1-x, 1-y, 1-z$	2.50	3.140(12)	123
C(18)–H(18)...O(9)	0.99	$-1+x, y, z$	2.59	3.574(13)	170
C(18)–H(18B)...O(10)	0.99		2.50	3.072(12)	116
IV					
O(16)–H(16A)...O(1)	0.85	$1-x, 1-y, 1-z$	2.07	2.822(8)	148
O(16)–H(16B)...N(7S)	0.85		1.90	2.689(8)	156
O(17)–H(17A)...N(4S)	0.85		2.38	3.171(11)	141
O(17)–H(17A)...O(2)	0.93	$-x, -y, 1-z$	2.46	3.346(14)	155
C(4)–H(4)...O(5)	0.96	$-x, -y, -z$	2.40	3.251(11)	149
C(3S)–H(3SA)...O(8)	0.93	$-x, 1-y, 1-z$	2.55	3.094(11)	114
C(8)–H(8)...O(12)	0.93	$1-x, 1-y, 1-z$	2.50	3.140(12)	123
C(9)–H(9)...N(1S)	0.93	$1-x, 1-y, 1-z$	2.59	3.574(13)	170
C(13)–H(13)...O(7)	0.93	$-x, 1-y, 1-z$	2.50	3.072(12)	116
C(14)–H(14)...O(4)	0.93	$-x, -y, 1-z$			

Table 4. Interactions N–O... π in the crystal packings of compounds **II** and **IV**

Interaction	O–Cg, Å	Symmetry code	Angle N–O...Cg, deg*
II			
N(1)–O(5)... π (Fur)	3.465(10)	$1 + x, 1/2 - y, 1/2 + z$	114.7(6)
N(2)–O(9)... π (Fur)	3.385(10)	$1 - x, 1 - y, 1 - z$	128.7(7)
N(3)–O(14)... π (Fur)	3.510(10)	$-x, 1 - y, 1 - z$	71.7(6)
IV			
N(1)–O(4)... π (Fur)	3.208(3)	$x, -1 + y, z$	105.0(2)
N(2)–O(9)... π (Fur)	3.341(3)	$-x, 1 - y, -z$	105.64(19)
N(3)–O(15)... π (Fur)	3.227(3)	$1 - x, -y, 1 - z$	116.9(2)

* Cg are centroids of aromatic rings.

Table 5. Results on antibacterial activity against *M. smegmatis*

Compound	MIC, nmol/disc	Inhibition zone, mm			Literature
		24 h	24 h	120 h	
I	2000	6.0 \pm 0.5*		0	
II	1500	6.0 \pm 0.5*		0	
IV	2000	6.6 \pm 0.5*		6.1 \pm 0.5*	
[Cu(Fur) ₂ (CH ₃ CN)]	280	6.5 \pm 0.5*		0	[21]
[Cu(Nfur) ₂ (H ₂ O) ₂]	1248	6.0 \pm 0.5*		0	[39]
[Cu(Fur) ₂ (Phen)]	4	7 \pm 0.5*		7 \pm 0.5*	[15]
[Zn(Fur) ₂ (Bpy)]	92	6.5 \pm 0.5		6.5 \pm 0.5	[16]
Hfur	55	7 \pm 0.5*		6 \pm 0.5*	
Hnfur	1000	6.2 \pm 0.5*		0	
INH	730	7.0 \pm 0.5		6.5* \pm 0.5	
Rif	6	6.5 \pm 0.5		6.5 \pm 0.5	

* The inhibition growth zone of the bacterial culture initially formed after several hours of growth begins to grow over the whole zone surface; empty rows mean that the inhibition zone is absent. 0—there is no growth inhibition zone of the bacterial strain.

CONFLICT OF INTEREST

The authors of this work declare that they have no conflicts of interest.

REFERENCES

1. Sessoli, R. and Powell, A.K., *Coord. Chem. Rev.*, 2009, vol. 253, p. 2328.
2. Layfield, R.A. and Murugesu, M., *Lanthanides and Actinides in Molecular Magnetism*, Wiley-VCH, 2015.
3. *Molecular Magnetic Materials*, Sieklucka, B. and Pinkowicz, D., Eds., Weinheim: Wiley-VCH, 2017.
4. Kiskin, M.A., Varaksina, E.A., Taydakov, I.V., and Eremenko, I.L., *Inorg. Chim. Acta*, 2018, vol. 482, p. 85.
5. Shmelev, M.A., Voronina, Y.K., Gogoleva, N.V., et al., *Russ. Chem. Bull.*, 2020, vol. 69, p. 1544. <https://doi.org/10.1007/s11172-020-2934-0>
6. Binnemans, K., *Chem. Rev.*, 2009, vol. 109, p. 4283.
7. Zhen-Feng Chen, Ming-Xiong Tan, Yan-Cheng Liu, et al., *J. Inorg. Biochem.*, 2011, vol. 105, p. 426.
8. Kaczmarek, M.T., Zabiszak, M., Nowak, M., and Jas-trzab, R., *Coord. Chem. Rev.*, 2018, vol. 370, p. 42.
9. Guan, Q.-L., Xing, Y.-H., Liu, J., et al., *J. Inorg. Biochem.*, 2013, vol. 128, p. 57.
10. Rashid, H.U., Martines, M.A.U., Jorge, J., et al., *Bio-organ. Med. Chem.*, 2016, vol. 4, p. 5663.
11. Bombieri, G., Artali, R., Mason, S.A., et al., *Inorg. Chim. Acta*, 2018, vol. 470, p. 433.
12. Babic, A., Vorobiev, V., Xayaphoummine, C., et al., *Chem.-Eur. J.*, 2018, vol. 24, p. 1348.
13. Phukan, B., Mukherjee, C., and Varshney, R., *Dalton Trans.*, 2018, vol. 47, p. 135.
14. Zhang, T., Zhu, X., Wong, W.-K., et al., *Chem.-Eur. J.*, 2013, vol. 19, p. 739.
15. Lutsenko, I.A., Baravikov, D.E., Kiskin, M.A., et al., *Russ. J. Coord. Chem.*, 2020, vol. 46, p. 411. <https://doi.org/10.1134/S1070328420060056>
16. Lutsenko, I.A., Yambulatov, D.S., Kiskin, M.A., et al., *Russ. J. Coord. Chem.*, 2020, vol. 46, p. 787. <https://doi.org/10.1134/S1070328420120040>

17. Lutsenko, I.A., Yambulatov, D.S., Kiskin, M.A., et al., *Chem. Select.*, 2020, vol. 5, p. 11837.
18. Lutsenko, I.A., Kiskin, M.A., Koshenskova, K.A., et al., *Russ. Chem. Bull.*, 2021, vol. 70, p. 463. <https://doi.org/10.1007/s11172-021-3109-3>
19. Uvarova, M.A., Lutsenko, I.A., Kiskin, M.A., et al., *Polyhedron*, 2021, vol. 203, p. 115241.
20. Lutsenko, I.A., Baravikov, D.E., Koshenskova, K.A., et al., *RSC Adv.*, 2022, vol. 12, p. 5173.
21. Lutsenko, I.A., Nikiforova, M.E., Koshekskova, K.A., et al., *Russ. J. Coord. Chem.*, 2021, vol. 47, p. 881. <https://doi.org/10.1134/S1070328421350013>
22. Bartolomé, E., Bartolomé, J., Arauz, A., et al., *J. Mater. Chem.*, 2016, vol. 22, p. 5038.
23. Li, X., Jin, L., Lu, S., and Zhang, J., *J. Mol. Struct.*, 2002, vol. 604, p. 65.
24. Bartolomé, E., Bartolomé, J., Arauzo, A., et al., *J. Mater. Chem.*, 2018, vol. 19, p. 5286.
25. Li, X., Zheng, X., Jin, L., and Zhang, J., *J. Mol. Struct.*, 2001, vol. 559, p. 341.
26. Bartolomé, E., Bartolomé, J., Melnic, S., et al., *Dalton Trans.*, 2019, vol. 42, p. 10153.
27. Uvarova, M.A., Lutsenko, I.A., Nikiforova, M.E., et al., *Russ. J. Coord. Chem.*, 2022, vol. 48, p. 457. <https://doi.org/10.1134/S1070328422080073>
28. Li, Xia, Bel'skii, V.K., Dement'ev, A.I., and Medvedev, Yu.N., *Russ. J. Inorg. Chem.*, 2004, vol. 49, p. 386.
29. Krause, L., Herbst-Irmer, R., Sheldrick, G.M., and Stalke, D., *J. Appl. Crystallogr.*, 2015, vol. 48, p. 3.
30. Sheldrick, G.M., *Acta Crystallogr., Sect. A: Found. Adv.*, 2015, vol. 71, p. 3.
31. Dolomanov, O.V., Bourhis, L.J., Gildea, R.J., et al., *J. Appl. Crystallogr.*, 2009, vol. 42, p. 339.
32. Casanova, D., Llunell, M., Alemany, P., and Alvarez, S., *Chem.-Eur. J.*, 2005, vol. 11, p. 1479.
33. Lam, A.W.H., Wong, W.T., Gao, S., et al., *Eur. J. Inorg. Chem.*, 2003, vol. 2003, p. 149.
34. Singh, U.P., Kumar, R., and Upreti, S., *J. Mol. Struct.*, 2007, vol. 831, p. 97.
35. Liu, B.X., Chen, G.H., and Zhang, L.J., *Acta Crystallogr., Sect. E: Struct. Rep. Online*, 2007, vol. 63, p. 2263.
36. Sharma, S., Yawer, M., Kariem, M., et al., *Russ. J. Coord. Chem.*, 2015, vol. 41, no. 7, p. 469.
37. Arıcı, C., Ülkü, D., Tahir, M.N., et al., *Acta Crystallogr., Sect. C: Cryst. Struct. Commun.*, 1999, vol. 55, p. 198.
38. Kepert, C.J., Wei-Min, L., Junk, P.C., et al., *Aust. J. Chem.*, 1999, vol. 52, p. 459.
39. Koshenskova, K.A., Lutsenko, I.A., Nelyubina, Y.V., et al., *Russ. J. Inorg. Chem.*, 2022, vol. 67, no. 2, p. 1545. <https://doi.org/10.1134/S003602362270005X>

Translated by E. Yablonskaya